A Predictive Model for Lymph Node Involvement with Malignancy on PET/CT in Non–Small-Cell Lung Cancer

Malcolm D. Mattes, MD, Wolfgang A. Weber, MD,† Amanda Foster, MS,‡ Ariella B. Moshchinsky, BS,§ Salma Ahsanuddin, BS,§ Zhigang Zhang, PhD,‖ Weiji Shi, MS,‖ Nabil P. Rizk, MD,¶ Abraham J. Wu, MD,‡ Hani Ashamalla, MD,§ and Andreas Rimner, MD‡*

Introduction: Accurate assessment of lymph node (LN) involvement with malignancy is critical to staging and management of non–small-cell lung cancer. The goal of this retrospective study was to determine the tumor and imaging characteristics independently associated with malignant involvement of LNs visualized on positron emission tomography/computed tomography (PET/CT).

Methods: From 2002 to 2011, 172 patients with newly diagnosed non–small-cell lung cancer underwent PET/CT within 31 days before LN biopsy. Among these patients, 504 anatomically defined, pathology-confirmed LNs were visualized on PET/CT. Logistic regression analysis was used to determine the associations between nodal involvement with malignancy and several clinical and imaging variables, including tumor histology, tumor grade, LN risk category in relation to the primary tumor location, pathologic findings from additional biopsied LNs, interval between PET/CT and biopsy, primary tumor largest dimension, primary tumor standardized uptake value (SUV_{max}), LN short-axis dimension, and LN SUV_{max}.

Results: On univariate analysis, adenocarcinoma histology ($p = 0.010$), high LN risk category ($p < 0.001$), larger LN short-axis dimension ($p < 0.001$), and higher LN SUV_{max} ($p < 0.001$) all correlated with nodal involvement. On multivariate analysis, adenocarcinoma histology ($p = 0.003$), high LN risk category ($p = 0.005$), and higher LN SUV_{max} ($p < 0.001$) correlated with nodal involvement, whereas LN short-axis dimension was no longer statistically significant ($p = 0.180$). A nomogram developed for clinical application based on this analysis had excellent concordance between predicted and observed results (concordance index, 0.95).

Conclusion: Adenocarcinoma histology, higher LN SUV_{max}, and higher LN risk category independently correlate with nodal involvement with malignancy and may be used in a model to accurately predict the risk of a node's involvement with malignancy.

*Department of Radiation Oncology, West Virginia University, Morgantown, West Virginia; Departments of †Radiology and ‡Radiation Oncology, Memorial Sloan-Kettering Cancer Center, New York, New York; §Department of Radiation Oncology, New York Methodist Hospital, Brooklyn, New York; and Departments of ‖Epidemiology and Biostatistics and ¶Surgery, Memorial Sloan-Kettering Cancer Center, New York, New York.

Disclosure: The authors declare no conflict of interest.

Address for correspondence: Andreas Rimner, MD, Department of Radiation Oncology, Memorial Sloan-Kettering Cancer Center, 1275 York Avenue, New York, NY 10065. E-mail: rimnera@mskcc.org

DOI: 10.1097/JTO.0000000000000601

ISSN: 1556-0864/15/1008-1207

Key Words: NSCLC, PET, Staging, Lymph node.

(*J Thorac Oncol.* 2015;10: 1207–1212)

Lymph node (LN) staging is an important component of the workup of patients with non–small-cell lung cancer (NSCLC), as it affects prognosis and guides management.[1] Although 18F-fluorodeoxyglucose (FDG) positron emission tomography/computed tomography (PET/CT) is the most accurate imaging modality for LN staging, it is still not considered accurate enough to forego pathologic confirmation of nodal involvement with malignancy.[2] Common procedures for obtaining LN pathology such as mediastinoscopy and endobronchial ultrasound-guided biopsies are limited, although, in terms of the stations of nodes that can be accessed in a single procedure, and as such, improving the accuracy of imaging techniques is also crucial in guiding the surgical approach. Moreover, for the many patients with NSCLC who are medically inoperable with significant comorbidities that limit the feasibility of safely performing an invasive procedure because of the risk of complications, improving noninvasive, imaging-based approaches to predict the nodal involvement with malignancy would expedite definitive management of their disease and improve radiation therapy target volume delineation, potentially sparing patients from the toxicity associated with a larger treatment volume while enabling treatment of gross disease to high doses.[3–5]

Multiple studies have attempted to predict nodal involvement with malignancy based on a variety of size and/or SUV criteria using imaging modalities such as CT, PET, or PET/CT. These studies generally can be divided into those assessing individual nodes based strictly on the imaging characteristics of that node and those assessing the risk to a more global LN region based on the types of primary tumor-specific factors, for instance determining the incidence of occult mediastinal LN positivity in patients with a clinically negative mediastinum on PET and/or CT. Regarding the former, the reported ranges for sensitivity and specificity for individual LNs based on the size or SUV criteria are wide, because the studies were performed in different patient populations and used different criteria for malignancy to increase either the sensitivity or the specificity of the imaging test.[6–14] Regarding the latter, there are conflicting data on which factors are most important in predicting mediastinal spread, depending on a multitude of

factors including the type of imaging used, surgical techniques, and how one defines nodal positivity on imaging alone.[15–24] In this study, we sought to synthesize these concepts to determine which tumor and imaging characteristics are independently associated with involvement of specific pathologically confirmed LNs to develop a more accurate predictive tool to improve noninvasive nodal evaluation in NSCLC.

PATIENTS AND METHODS

This study retrospectively assessed 504 LNs from 172 patients, which were both biopsied and visualized on a prebiopsy PET/CT. Patients were identified for inclusion from the charts of 729 consecutive patients with newly diagnosed NSCLC who underwent pathologic LN staging at Memorial Sloan-Kettering Cancer Center (MSKCC) from 2002 to 2011 and PET/CT within 31 days before biopsy. Only LNs that were anatomically defined at the time of biopsy according to their LN station were included in this analysis, because this information was used to identify the biopsied node on PET/CT. Any biopsied LNs for which no visible LN could be identified in the station of interest on PET/CT were excluded. Conversely, if more than one LN could be visualized in a station of interest, the imaging characteristics of the largest LN in that region were recorded.

Patients with a history of previous chemotherapy, radiation therapy, granulomatous disease, or nonskin cancer malignancy were excluded. Nodal pathology could be obtained by any means, including excisional biopsy (by means of mediastinoscopy, thoracotomy, etc.) or minimally invasive biopsy/needle aspiration (by means of bronchoscopy, endobronchial ultrasound, etc.). The selection of LNs to biopsy was at the discretion of the clinician performing the biopsy, but it was not restricted to LNs that appeared malignant on imaging, because many LN stations were biopsied as part of the clinician's standard staging evaluation of the patient. Given the retrospective nature of this study, no further information was readily available to explain the rationale for each individual biopsy.

The PET/CT scans were carried out on a variety of scanner models, both within our institution and at outside hospitals or imaging centers. More than 15 scanner types/models were used among the patients included in this study. For the patients who underwent PET/CT at MSKCC, patient preparation and image acquisition protocols were comparable over the years. Patients were instructed to fast for at least 6 hours before FDG administration, and blood glucose levels were required to be less than 200 mg/dl at the time of injection. The scans were acquired from the upper thighs to the base of the skull (5–7 bed positions) 60 to 90 minutes after injection of approximately 400 MBq FDG. CT was performed for attenuation correction and anatomical localization. Immediately after the CT image acquisition, PET data were acquired for 3 to 5 minutes per bed position. The attenuation-corrected PET data were reconstructed using an ordered-subset expectation maximization iterative reconstruction. All raw Digital Imaging and Communications in Medicine files from scans at our center and outside institutions were imported into the AW Volume Viewer software (GE Healthcare, Pittsburgh, PA) without adjustments for differing scanner and protocol methods. All images were re-reviewed for the purpose of this study using the AW Volume Viewer software to verify and remeasure the results initially reported by a board-certified nuclear medicine radiologist. Parameters that were remeasured included the primary tumor largest dimension, primary tumor SUV_{max}, LN short-axis dimension, and LN SUV_{max}. SUV_{max} was defined as the highest FDG uptake within a region of interest that encompassed a given lesion, as defined according to PET response criteria in solid tumors (PERCIST) criteria.[25]

Univariate logistic regression analysis was used to determine whether there was an association between nodal involvement with malignancy and several clinical and imaging variables, including tumor histology, tumor grade, LN risk category (as defined in Table 1), pathologic findings from any additional biopsied LNs, interval between PET/CT and biopsy, PET/CT location, primary tumor largest dimension, primary tumor SUV_{max}, LN short-axis dimension, and LN SUV_{max}. Of note, LN risk categories based on the primary tumor location were based on the patterns of nodal spread as described in previous surgical series.[16,26–29] Factors with a p value less than 0.05 on univariate analysis were included in the multivariate logistic regression model. A nomogram for predicting LN involvement with malignancy based on the aforementioned multivariate analysis was developed for clinical application. Concordance index (c-index) was calculated for the multivariate model, which was used to estimate the probability of concordance between predicted and observed responses. The c-index ranges from 0.5 to 1.0, with a value of 0.5 indicating that the model is no better than chance, and a value of 1.0 indicating perfect discrimination. Internal cross-validation of the predictive model was performed using the Jackknife (leave-one-out) method, with Hosmer–Lemeshow goodness-of-fit statistic computed to examine the calibration of the model. Statistical analysis was performed using the software SAS version 9.2 (SAS Institute, Inc. Cary, NC). This study was approved by the MSKCC institutional review board (WA0099-13) and was performed following the ethical principles of the Declaration of Helsinki.

RESULTS

The median age of the 172 patients who met our criteria for analysis was 67.1 years (range, 43.6–97.3 years), and 90% were either current or former smokers. The characteristics of their primary tumors are shown in Table 2. The median primary tumor size in the single largest dimension was 2.8 cm

TABLE 1. Definition of Lymph Node Risk Categories

	High	Intermediate	Low
RUL	10–14R, 4R	1R, 2R, 3, 7, 8, 9	1L, 2L, 4L, 5, 6, 10L
RML	10–14R, 4R, 7	1R, 2R, 3, 8, 9	1L, 2L, 4L, 5, 6, 10L
RLL	10–14R, 4R, 7	1R, 2R, 3, 8, 9	1L, 2L, 4L, 5, 6, 10L
LUL	10–14L, 4L, 5, 6	1L, 2L, 3, 7, 8, 9	1R, 2R, 4R, 10R
LLL	10–14L, 4L, 7	1L, 2L, 3, 5, 6, 8, 9	1R, 2R, 4R, 10R

LLL, left lower lobe; LUL, left upper lobe; RML, right middle lobe; RLL, right lower lobe; RUL, right upper lobe.

TABLE 2. Primary Tumor Characteristics

Characteristic	*n* (%)
Tumor histology	
Adenocarcinoma	104 (59)
Squamous cell carcinoma	54 (31)
Other/unclassified	14 (8)
Tumor location	
Right upper lobe	68 (39)
Right middle lobe	9 (5)
Right lower lobe	34 (20)
Left upper lobe	36 (21)
Left lower lobe	25 (15)
Tumor grade	
Well differentiated	4 (2)
Moderately differentiated	65 (38)
Poorly differentiated	93 (54)
Unknown	10 (6)

(range, 0.4–12.0 cm), and the median primary tumor SUV_{max} was 10.5 (range, 0.4–44.4).

The mean interval between PET/CT and LN biopsy was 15.8 days (standard deviation, 8.5 days). The PET/CT was performed at our institution in 77% of patients and at an outside institution in 23% of patients. The characteristics of the 504 evaluated LNs are shown in Table 3. The median LN short-axis size was 0.7 cm (range, 0.3–4.7 cm), and the median SUV_{max} was 2.1 (range, 0.5–20.3). Among the pathologically positive nodes (n = 68), the median SUV_{max} was 6.2 (range, 1.5–20.3), and eight nodes (11.8%) had SUV_{max} less than 3.0.

According to the univariate analysis in Table 4, adenocarcinoma (versus squamous cell) histology, high (versus low to intermediate) LN risk category, larger LN short-axis dimension, higher LN SUV_{max}, and PET/CT scan from an outside institution all correlated with a higher odds ratio for nodal involvement with malignancy. Factors that failed to demonstrate significant association on univariate analysis included tumor grade, interval between PET/CT and biopsy, primary tumor size, and primary tumor SUV_{max}. According to the multivariate analysis, adenocarcinoma histology, high LN risk category, higher LN SUV_{max}, and PET/CT scan from an outside institution all correlated with a higher odds ratio for nodal involvement with malignancy, whereas the association with LN short-axis dimension was no longer statistically significant. Of note, the location of PET/CT was not included in the final model (Table 5), because it has no clinical relevance to patients and physicians not limited to our center. Its inclusion only marginally increased the c-index from 0.950 to 0.955. A nomogram for predicting LN involvement with malignancy based on the results of the multivariate analysis is shown in Figure 1. The c-index for the multivariate model was 0.95. A calibration curve validating model performance is shown in Figure 2. The Hosmer–Lemeshow goodness-of-fit test showed no significant difference between observed and expected nodal involvement with malignancy (p = 0.68). The c-index of the validation model was 0.87, indicating good discrimination.

TABLE 3. Lymph Node Characteristics

Characteristic	*n* (%)
Lymph node station	
Station 1–3	12 (2)
Station 4	224 (44)
Station 5–6	22 (4)
Station 7	131 (26)
Station 8–9	29 (6)
Station 10–14	86 (17)
Means of obtaining pathology	
Excision by thoracotomy	112 (22)
Excision by mediastinoscopy	355 (70)
Fine-needle aspiration	37 (7)
Lymph node histology	
Benign	436 (86)
Malignant	68 (14)
Additional biopsied lymph node(s)	
Negative	376 (75)
>1 positive	95 (19)
Unknown	33 (7)
LN risk category	
High	227 (45)
Intermediate	171 (34)
Low	106 (21)

LN, lymph node.

DISCUSSION

In this study, we have shown that a combination of clinical and imaging characteristics can be used to accurately predict nodal involvement with malignancy in patients with newly diagnosed NSCLC. Adenocarcinoma histology, higher LN SUV_{max}, and higher LN risk category in relation to the primary tumor site were all independently associated with nodal positivity. Given the large number of nodes assessed in this study, the final model may serve as a powerful tool in guiding the approach to pathologic nodal staging and improving noninvasive assessment in those patients receiving nonsurgical management of their disease.

Several previous studies have explored predictive models for nodal involvement in NSCLC, primarily in the context of determining the risk factors for any mediastinal LN involvement with malignancy in patients with a clinically negative mediastinum on PET or CT.[15–24] This should be distinguished from our approach, in which specific LNs visible on imaging were assessed for the probability of their involvement with malignancy, with the goal being more accurate classification of nodes that are otherwise challenging to interpret based on the commonly used PET or CT criteria alone. With this distinction in mind, it is not surprising that characteristics of the primary tumor such as size and SUV_{max}, which have been demonstrated to predict for a higher global risk of LN involvement in previous studies, were not as predictive of involvement of specific LNs as the qualities of that LN itself in our study. The ability of SUV_{max} of the primary tumor to predict for occult nodal involvement with malignancy is controversial

TABLE 4. Univariate Logistic Regression Analysis of the Relationship between Clinical Characteristics and PET Parameters with Nodal Involvement with Malignancy

Factor	Odds Ratio (95% CI)	*p* Value
Tumor histology		
Squamous cell	1.00 (reference)	
Adenocarcinoma	2.29 (1.20–4.34)	0.01
Other	0.83 (0.23–3.06)	0.78
Tumor grade		
Well	0.29 (0.04–2.25)	0.24
Moderate	0.78 (0.45–1.34)	0.36
Poor	1.00 (reference)	
Not reported	0.70 (0.20–2.42)	0.57
Lymph node risk category		
High	1.00 (reference)	
Low to intermediate	0.15 (0.08–0.29)	<0.01
Additional biopsied LN(s)		
Negative	1.00 (reference)	
Positive (≥1)	1.55 (0.78–3.05)	0.21
PET/CT location		
MSKCC	1.00 (reference)	
Outside institution	2.48 (1.45–4.25)	<0.01
Interval from PET/CT to biopsy (days)	0.99 (0.96–1.02)	0.63
Primary tumor largest dimension (cm)	0.91 (0.79–1.04)	0.16
Primary tumor SUV_{max}	0.97 (0.94–1.01)	0.13
Lymph node short-axis dimension (cm)	17.52 (8.90–34.49)	<0.01
Lymph node SUV_{max}	2.17 (1.82–2.58)	<0.01

CI, confidence interval; CT, computed tomography; LN, lymph node; MSKCC, Memorial Sloan-Kettering Cancer Center; PET, positron emission tomography.

TABLE 5. Multivariate Logistic Regression Analysis of the Relationship between Clinical Characteristics and PET Parameters with Nodal Involvement with Malignancy

Factor	Odds Ratio (95% CI)	*p* Value
Tumor histology		
Squamous cell	1.00 (reference)	
Adenocarcinoma	5.04 (1.76–14.48)	<0.01
Other	3.40 (0.46–25.45)	0.23
Lymph node risk category		
High	1.00 (reference)	
Low to intermediate	0.28 (0.12–0.68)	<0.01
Lymph node SUV_{max}	2.00 (1.64–2.44)	<0.01
Lymph node short-axis dimension (cm)	1.76 (0.77–3.99)	0.18

CI, confidence interval; PET, positron emission tomography.

in itself, because two recent studies from large academic centers have conflicting findings.[15,24] Given that SUV is a function of tumor size and histology, this inconsistency may stem from variability in the patient populations evaluated in different studies. Trister et al. also did not include the primary tumor size as an independent variable during analysis, which limits its interpretability. However, our findings do agree with the majority of the published literature in implicating adenocarcinoma histology as a risk factor for LN involvement with malignancy.[16–18]

Primary tumor location has often been associated with the risk of LN involvement with malignancy, although the highest risk location was the upper lobes in some studies,[17,18] the upper or middle lobes in another study,[16] and central location irrespective of lobe in other studies.[18,21,23] Given that our study evaluated specific nodal stations rather than the risk for any mediastinal involvement, we took a slightly different approach, defining the LN risk categories based on the known patterns of occult nodal spread[16,26–29] and found that this categorization was independently predictive of the presence of metastasis in a given LN in question.

Somewhat unexpectedly, LN short-axis dimension was not associated with nodal involvement with malignancy on multivariate analysis. Although the reason for this is not entirely clear, it may be due to strong associations between LN short-axis dimension and other factors that were included in the model, such as LN risk category and SUV_{max}. It could also be related to the fact that most of the LNs evaluated in this study were pathologically benign, and as such the median LN short-axis dimension was relatively small. With less measured variability in LN size, the multivariate model may not have been adequately powered to detect a difference. Although LN short-axis dimension made negligible impact on the predictive power of the nomogram, we elected to include it in the final prediction model because clinically LN size has been consistently used in predicting the risk of nodal malignancy in the pre-PET era, albeit as a relatively unreliable parameter.[6]

Finally, there is conflicting evidence for whether clinically positive hilar LNs on PET is a risk factor for mediastinal involvement.[15–18] In a recent large series, Farjah et al.[15] actually found that for patients with clinical stage T1-2 N0-1 NSCLC by PET/CT, only clinically positive hilar nodal involvement was correlated with pathologic mediastinal LN involvement, whereas primary tumor location, size, histology, and SUV_{max}, and extent of nodal disease on CT were not associated with pathologic mediastinal LN involvement. Similarly, Dooms et al.[30] also recently reported that 24% of patients who were clinically N1 based on the PET harbored pathologic mediastinal LN malignancy. Interestingly, our model did not show that the pathologic status of additional biopsied LNs (hilar or mediastinal) correlated with the status of a node in question. This discrepancy may be because we strictly included only pathologic information in this analysis so as to avoid any uncertainty associated with interpretation of hilar LN involvement based on the imaging alone or because these previous publications inconsistently report the criteria for clinically defining hilar nodal involvement on PET or CT, or the elapsed time from imaging to pathologic assessment, all of which would impact the outcome of the study.

There are several important limitations to this study. First, we relied on accurate documentation of nodal station on the biopsy report to identify and correlate the pathologic findings with the imaging findings, an approach which will inevitably lead to some misclassification, perhaps more so for

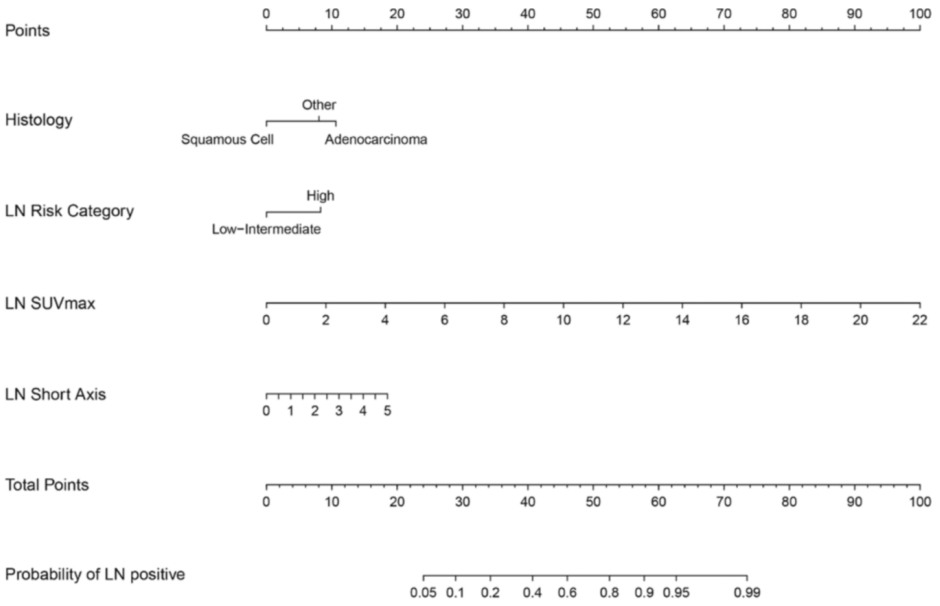

FIGURE 1. Nomogram for predicting lymph node (LN) involvement with malignancy based on the multivariate analysis in Table 5.

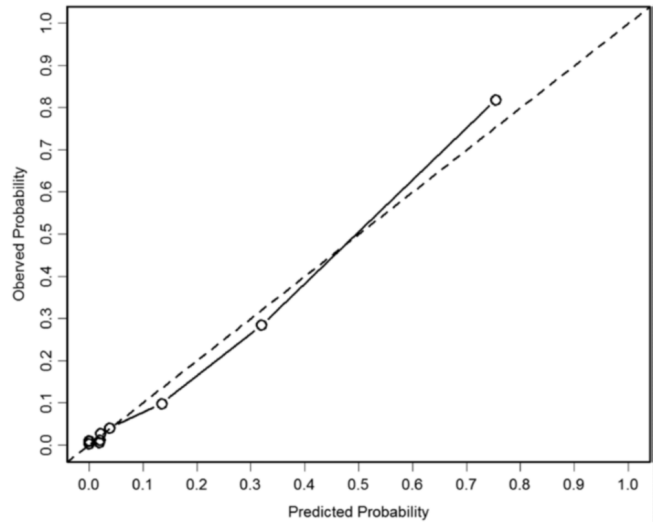

FIGURE 2. Calibration plot comparing observed and predicted probabilities of nodal involvement with malignancy (c-index, 0.87; Hosmer–Lemeshow goodness-of-fit test, $p = 0.68$).

hilar than mediastinal nodal stations. We attempted to minimize this by excluding any stations for which there was no clearly identifiable node and recording data for only the largest node in a given station with multiple visible nodes, because this would generally be the node most likely to be surgically or endoscopically accessible for biopsy. Another source of bias may lie in the nodes that were selected for biopsy, because some of these were biopsied based on the physician's standard evaluation rather than any abnormality on CT or PET. Needle aspiration by endobronchial ultrasound-guided transbronchial lymph node aspiration was performed in a minority of patients in our study, but it is known to be associated with false-negative nodal pathology due to insufficient tissue sampling at a rate of approximately 10%.[28] Finally, although the inclusion of outside scans in this study may be viewed as a limitation due to subtle variations in image acquisition and reconstruction procedures, we would argue that this may make our findings more generalizable. PET/CT location at an outside institution was associated with nodal positivity, but this is most likely related to other factors, for instance differences in the presentation, workup, or management of patients, or referral bias for patients with more advanced disease. These limitations should be carefully weighed against the strengths of our data, which include the assessment of a larger number of LNs than most studies of this kind and the strict use of pathologic information rather than clinical nodal assessment to guide our analysis.

CONCLUSION

Adenocarcinoma histology, higher LN SUV_{max}, and higher LN risk category independently correlate with nodal involvement with malignancy and may be used in a model to accurately predict the risk of a node's involvement with malignancy.

ACKNOWLEDGMENTS

This work was in part supported by an NIH Core Grant P30 CA008748 (to Zhigang Zhang and Weiji Shi).

REFERENCES

1. Mountain CF, Dresler CM. Regional lymph node classification for lung cancer staging. *Chest* 1997;111:1718–1723.
2. National Comprehensive Cancer Network® (NCCN). *Practice Guidelines in Oncology: Non-Small Cell Lung Cancer, Version 2, 2013*. Available at: www.nccn.org. Accessed December 15, 2014.
3. Rosenzweig KE, Sura S, Jackson A, Yorke E. Involved-field radiation therapy for inoperable non small-cell lung cancer. *J Clin Oncol* 2007;25:5557–5561.
4. Yu JM, Sun XD, Li MH, et al. [Involved-field three-dimensional conformal radiation treatment for stage III non-small-cell lung]. *Zhonghua Zhong Liu Za Zhi* 2006;28:526–529.
5. De Ruysscher D, Nestle U, Jeraj R, Macmanus M. PET scans in radiotherapy planning of lung cancer. *Lung Cancer* 2012;75:141–145.

6. Toloza EM, Harpole L, Detterbeck F, McCrory DC. Invasive staging of non-small cell lung cancer: a review of the current evidence. *Chest* 2003;123(1 Suppl):157S–166S.
7. Lv YL, Yuan DM, Wang K, et al. Diagnostic performance of integrated positron emission tomography/computed tomography for mediastinal lymph node staging in non-small cell lung cancer: a bivariate systematic review and meta-analysis. *J Thorac Oncol* 2011;6:1350–1358.
8. Truong MT, Viswanathan C, Erasmus JJ. Positron emission tomography/computed tomography in lung cancer staging, prognosis, and assessment of therapeutic response. *J Thorac Imaging* 2011;26:132–146.
9. Ibeas P, Cantos B, Gasent JM, Rodríguez B, Provencio M. PET-CT in the staging and treatment of non-small-cell lung cancer. *Clin Transl Oncol* 2011;13:368–377.
10. Hellwig D, Graeter TP, Ukena D, et al. 18F-FDG PET for mediastinal staging of lung cancer: which SUV threshold makes sense? *J Nucl Med* 2007;48:1761–1766.
11. Lee BE, Redwine J, Foster C, et al. Mediastinoscopy might not be necessary in patients with non-small cell lung cancer with mediastinal lymph nodes having a maximum standardized uptake value of less than 5.3. *J Thorac Cardiovasc Surg* 2008;135:615–619.
12. Wang J, Welch K, Wang L, Kong FM. Negative predictive value of positron emission tomography and computed tomography for stage T1-2N0 non-small-cell lung cancer: a meta-analysis. *Clin Lung Cancer* 2012;13:81–89.
13. Billé A, Pelosi E, Skanjeti A, et al. Preoperative intrathoracic lymph node staging in patients with non-small-cell lung cancer: accuracy of integrated positron emission tomography and computed tomography. *Eur J Cardiothorac Surg* 2009;36:440–445.
14. Gould MK, Kuschner WG, Rydzak CE, et al. Test performance of positron emission tomography and computed tomography for mediastinal staging in patients with non-small-cell lung cancer: a meta-analysis. *Ann Intern Med* 2003;139:879–892.
15. Farjah F, Lou F, Sima C, Rusch VW, Rizk NP. A prediction model for pathologic N2 disease in lung cancer patients with a negative mediastinum by positron emission tomography. *J Thorac Oncol* 2013;8:1170–1180.
16. Kanzaki R, Higashiyama M, Fujiwara A, et al. Occult mediastinal lymph node metastasis in NSCLC patients diagnosed as clinical N0-1 by preoperative integrated FDG-PET/CT and CT: risk factors, pattern, and histopathological study. *Lung Cancer* 2011;71:333–337.
17. Lee PC, Port JL, Korst RJ, Liss Y, Meherally DN, Altorki NK. Risk factors for occult mediastinal metastases in clinical stage I non-small cell lung cancer. *Ann Thorac Surg* 2007;84:177–181.
18. Al-Sarraf N, Aziz R, Gately K, et al. Pattern and predictors of occult mediastinal lymph node involvement in non-small cell lung cancer patients with negative mediastinal uptake on positron emission tomography. *Eur J Cardiothorac Surg* 2008;33:104–109.
19. Defranchi SA, Cassivi SD, Nichols FC, et al. N2 disease in T1 non-small cell lung cancer. *Ann Thorac Surg* 2009;88:924–928.
20. Park HK, Jeon K, Koh WJ, et al. Occult nodal metastasis in patients with non-small cell lung cancer at clinical stage IA by PET/CT. *Respirology* 2010;15:1179–1184.
21. Zhang Y, Sun Y, Xiang J, Zhang Y, Hu H, Chen H. A prediction model for N2 disease in T1 non-small cell lung cancer. *J Thorac Cardiovasc Surg* 2012;144:1360–1364.
22. Koike T, Koike T, Yamato Y, Yoshiya K, Toyabe S. Predictive risk factors for mediastinal lymph node metastasis in clinical stage IA non-small-cell lung cancer patients. *J Thorac Oncol* 2012;7:1246–1251.
23. Shafazand S, Gould MK. A clinical prediction rule to estimate the probability of mediastinal metastasis in patients with non-small cell lung cancer. *J Thorac Oncol* 2006;1:953–959.
24. Trister AD, Pryma DA, Xanthopoulos E, Kucharczuk J, Sterman D, Rengan R. Prognostic value of primary tumor FDG uptake for occult mediastinal lymph node involvement in clinically N2/N3 node-negative non-small cell lung cancer. *Am J Clin Oncol* 2014;37:135–139.
25. Wahl RL, Jacene H, Kasamon Y, Lodge MA. From RECIST to PERCIST: evolving considerations for PET response criteria in solid tumors. *J Nucl Med* 2009;50(Suppl 1):122S–150S.
26. Naruke T, Tsuchiya R, Kondo H, Nakayama H, Asamura H. Lymph node sampling in lung cancer: how should it be done? *Eur J Cardiothorac Surg* 1999;16(Suppl 1):S17–S24.
27. Kotoulas CS, Foroulis CN, Kostikas K, et al. Involvement of lymphatic metastatic spread in non-small cell lung cancer accordingly to the primary cancer location. *Lung Cancer* 2004;44:183–191.
28. Cerfolio RJ, Bryant AS. Distribution and likelihood of lymph node metastasis based on the lobar location of nonsmall-cell lung cancer. *Ann Thorac Surg* 2006;81:1969–1973; discussion 1973.
29. Navani N, Spiro SG, Janes SM. Mediastinal staging of NSCLC with endoscopic and endobronchial ultrasound. *Nat Rev Clin Oncol* 2009;6:278–286.
30. Dooms C, Tournoy KG, Schuurbiers O, et al. Endosonography for mediastinal nodal staging of clinical N1 non-small cell lung cancer: a prospective multicenter study. *Chest* 2015;147:209–215.